IASS 2018 BOSTON, JULY 16-20
CREATIVITY IN STRUCTURAL DESIGN

Proceedings of the IASS Symposium 2018
Creativity in Structural Design
July 16-20, 2018, MIT, Boston, USA
Caitlin Mueller, Sigrid Adriaenssens (eds.)

Ceramic Tectonics: Tile Grid Shell

Zach SEIBOLD*, Olga MESA[a], Milena STAVRIC[b], Martin BECHTHOLD

*Material Processes and Systems Group, Harvard Graduate School of Design
48 Quincy St, Cambridge MA 02138
zseibold@gsd.harvard.edu

[a] Roger Williams University, Material Processes and Systems Group, Harvard Graduate School of Design
[b] Graz University of Technology

Abstract

Funicular grid shells are typically constructed from steel or timber struts, but no examples are known using structural ceramics, a material known for its longevity and fire resistance. We report a method for the design and fabrication of a novel grid shell structure from unreinforced ceramic tile with minimal use of metal fasteners. Full-scale studies tested joinery and connection details, large-scale mockups helped to verify the assembly sequence, and physical component tests determined allowable strength values for structural design. A novel assembly sequence allows each rib to be installed vertically from above, eliminating the need for mechanical connections between ribs. A prototypical grid shell spans 6m with grid members fabricated from two layers of 6mm thick ceramic tile.

Keywords: grid ~~s~~hell, kagome, structural ceramics, structural tile, digital workflow, prototyping

Figure 1: Ceramic tile grid shell installation

1. Introduction

Clay-based ceramics are one of humankind's oldest material systems, notable for their hardness, durability, fire resistance and wide array of finishes. New material processing and production technologies have enabled the development of ceramic elements capable of performing thermally, environmentally, and acoustically [1], [2]. A relatively recent development has been the manufacturing of tiles in sizes up to 3.6m by 1.2m, with thicknesses between 3mm and 20mm. These elements are currently used as non-structural surface finish, but earlier work by Harvard's MaP+S group demonstrated their ability to form self-supportive structures in the form of three 3.6m tall columns [3].

Conceiving these tiles as sheets opens up a host of applications, including primary structural uses like those for plywood or metal. The brittleness of ceramics and its poor tensile strength, however, require the development of structural design criteria and new construction strategies.

This paper presents design and construction methods for structural ceramic tile, developed through the design of a full-scale ceramic grid shell. Following the brief review of precedents in structural ceramics we present the design principles for a ceramic grid shell with a particular focus on connection design, construction sequence and member redundancy. Material testing is reported as a method to confirm structural design criteria that were then applied to the analysis of a small grid shell which was designed and built in 2018 in Valencia, Spain.

1.1 Ceramics and Shell Structures

Several precedents exist for the use of ceramics in structural shells. The construction techniques developed by Rafael Guastavino eliminated much of the formwork historically required for the erection of masonry vaulting systems, adhering two or more layers of tiles laid at differing orientations with a bonding agent [4]. -Uruguayan engineer Eladio Dieste created reinforced brick shells using a material system he referred to as "cerámica armada", or reinforced ceramic [6]. His daring shells relied on post-tensioning of brick-like ceramic tiles. This innovative material system "transformed our perception of brick as a traditional material associated with heavy, vertical construction elements into one that allows for extreme thinness and long spans" [6], [7]. Research by López López et al. has documented examples of similar techniques deployed in the mid-20th century [8]. More recent work by the BLOCK Research Group and others have adapted these techniques to more complex 3-dimensional forms [9], [10]. These examples presented thin structural ceramic surfaces and related form-finding approaches, but they are all characterized by the use of relatively small rectangular tiles bonded with mortar. Given the radically enhanced production capacity of the industry designers are now investigating the tectonics of thin ceramic tile.

1.2 Grid Shells

Grid shells include properties that pair well with the physical traits of large-format ceramic tile. These types of rigid spatial structures take on the form of a doubly- or single curved surface that is discretized into a grid pattern rather than a solid surface [11]. Grid shells are notable for their ability to achieve large spans relative to their material usage. They are able to achieve these structural efficiencies with discrete, often planar, elements rather than the continuous doubly-curved forms that are needed for traditional shells. There are numerous examples of grid shells constructed mostly from steel or timber struts, but no examples are known using structural ceramics [12].

2. Ceramic Shell Prototype

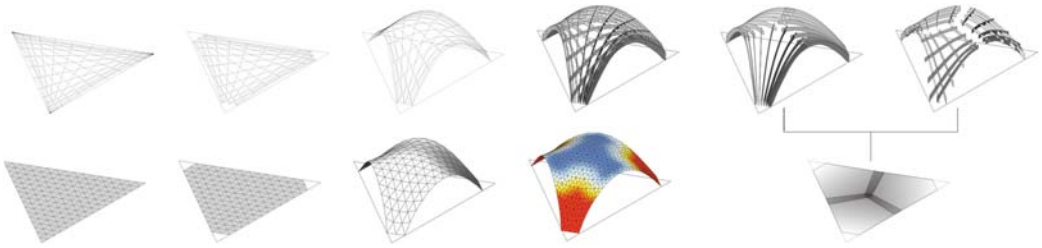

Figure 2: The form finding input and process, including steps for generating the initial shell form, generating and mapping a 2d kagome grid, and creating and discretizing ribs based on constructional logic.

The prototype ceramic grid shell presented here has been constructed at CEVISAMA 2018 in Valencia, Spain as a part of the Transhitos exhibition coordinated by Área de Hábitat del Instituto de Tecnología Cerámica (ITC). The prototype grid shell is a structure with a span of 6m, a maximum interior height of 2.48m, and an approximate occupiable interior area of 13.5sqm. It consists of 30 structural ribs comprised of 462 unique elements ranging from 820mm - 1810mm in length. The elements were cut from seventy-two 1.5m x 1.6m sheets of 6mm thick ceramic tile on a 2.5-axis CNC waterjet. The depth

of each element ranges from 180mm - 310mm, determined by a combination of structural and construction needs. Vertical slots are devised as the main connection strategy without using metal connectors. The slots lead to the effective structural depths being no less than 50% of the actual depth. The ceramic elements measure 107.22sqm in total surface area. The key design constraints were the mechanical properties of ceramics, the need for rapid assembly on-site, and the limited one-week duration of the exhibition.

2.1 Material Tests and Structural Design Values

ASTM test standards for thin tiles do not include mechanical properties for primary structural use. Structural safety factors are equally unknown. We are presenting three-point bending tests on laminated tiles, as well as tests of a double lap joint using mechanical connectors. The mechanical data from both tests was then used for the structural design of the prototypical grid shell.

2.1.1 Three-Point Bending Test

To verify the mechanical properties of the material, three-point bending tests were conducted with a thinner, 3mm tile, made from the same material, produced by the same manufacturer. A total of 14 samples were tested. The span was 300mm, the depth 40mm for one set and 50mm for another set. Each specimen consisted of four 3mm tiles, to a structural width of 12mm (Figure 3). Each specimen was tested as a single beam section. The average bending stress at fracture was 40.4 MPa (5,856psi, standard deviation 5.6 MPa), the average Young's Modulus at fracture was 13,924 MPa (2,020ksi, standard deviation 2,165 MPa). The stress values were consistent with data provided by the manufacturer. An initial safety factor of 33% was applied and maximum allowable stresses in bending of 27MPa (3,916psi) assumed for initial structural design studies.

2.1.2 Mechanical Joint Test

The team also conducted three-point bending tests to determine the capacity of a construction lap joint. A total of five samples were tested, with a span of 300mm and a depth 50mm. Each sample consisted of four 6mm tiles held such that areas of the four tiles overlapped in the middle. Here the tiles were mechanically connected using two M5 steel bolts placed in 6mm holes spaced 100mm apart on center. The test determined the peak load at fracture, which in turn allowed for the calculation of the equivalent bending stress in the material had the 4 tiles been continuous, thus without mechanical connection. The average bending stress based on peak load at fracture was 20.0 MPa (2903 psi, standard deviation 3.8 MPa), the average Young's Modulus at Fracture was 3,231 MPa (469 ksi, standard deviation 2,107 MPa). Both values are significantly lower than the equivalent values for continuous tiles without mechanical fasteners. Displacements at fracture were larger due to the slightly oversized bolt holes. Assuming a safety factor of 33% the allowable stresses in bending for a construction joint is 13.3MPa (1,929 psi).

Figure 3: Photograph of material test sample during three-point bending test.

2.2 Novel Design and Tectonic Strategies

2.2.1 Parametric Modeling Strategy

While material testing was ongoing a comprehensive parametric model was created that provided the flexibility of changing grid configuration and rib depth in response to production and structural

constraints, while allowing for a compressed fabrication and construction schedule. The model not only generated and analyzed the global geometry of the pavilion, it also served to discretize the form into components based on the size of available ceramic tile sheets, accommodate for assembly tolerances, size individual members for local load conditions, and generate toolpaths for fabrication. This functionality allowed for the adjustment of key design parameters to improve the global performance of the structure until late in the design process. The design team endeavored to reduce the number of independent parameters in the system, and designate as many geometric parameters as possible dependent on those independent input parameters. The main parameters driving the outcome of the parametric model included the span length and arch height of each opening, the thickness of the material stock, and the planometric arrangement of the grid pattern. A selected range of geometric and mechanical variables that were integrated into the model, and dependent on these base parameters is shown in Figure 4.

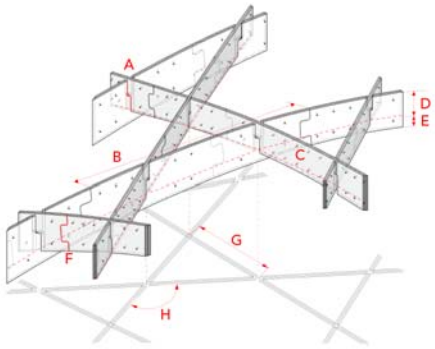

Figure 4: Geometric parameters of the ceramic grid shell system, including: A) Notch Orientation; B) Element Length; C) Spacing And Orientation Of Registration Holes; D) Base Structural Depth; E) Depth Increase Of Primary Elements; F) Notch Orientation And Scaling; G) Kagome Grid Density; H) Connection Angle

2.2.2 Plan Geometry: Projective Kagome Grid Pattern

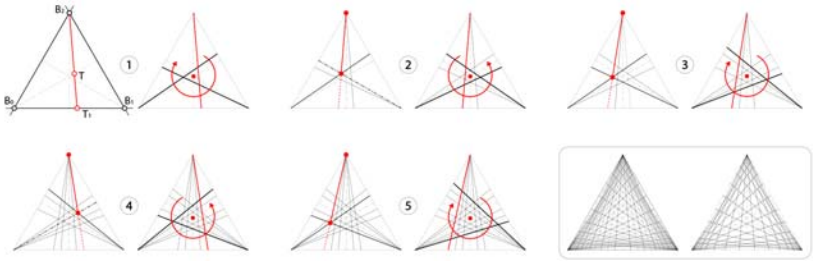

Figure 5: Parameters describing construction of the planometric geometry of the prototype, showing the first five steps of the process, and the completed grid. The location of parameter *T* determines the pattern density the grid.

The designers employed a trihexagonal tiling pattern - also known as a kagome grid pattern - in the planometric organization of the prototype grid shell (Figure 5). Kagome grid patterns can be found in traditional Japanese basketry, and, at the architectural scale, were employed in Shigeru Ban's Oita Prefectural Art Museum, and Centre Pompidou in Metz [13]. When applied to the form of a funicular shell, the kagome grid pattern allows for simple connections, as each node has the same valence as quadrilateral grid shell, while the triangulated zones of the pattern provide in-plane stiffness. A quadrangular grid pattern would have relied on the bending stiffness of connections at nodes, while a stiffer triangulated grid pattern would have increased the complexity of connections at nodes due to the higher valence of the base mesh. The structural performance of the kagome grid pattern in comparison to a quadrilateral grid pattern has been explored previously and found to have a superior bearing capacity [14][15].

In the case of the prototype, the kagome grid pattern was applied to a planar projective coordinate system, enabling each of the three primary spanning directions of the system to align with one of the

three support points. The coordinate system is defined by three points at the corners of one equilateral triangle, and a fourth point T, which must not lay on one of the edges and defines with point T_1 the density of the grid pattern. This configuration can be interpreted as a planar projective coordinate system with base points B_0, B_1, B_2, T. B0 is the origin of the projective coordinate system, connection B_1B_2 is the line at infinity and T_1 is the unit point of the projective plane [16].

The geometric characteristics of the organizational strategy described above provided several advantages. The closely spaced ribs near the supports provide structural redundancy in case one or several ribs break. The low node valence and inherent stiffness of the pattern permitted the use of simple, notched connections that are able to be assembled without mechanical fasteners.

2.2.3 Structural Rib Design

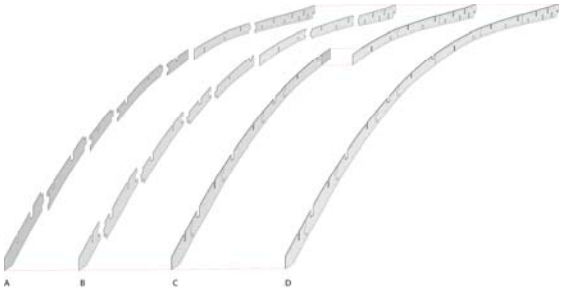

Figure 6: Drawing showing the assembly process of a typical rib, showing two staggered layers (A, B) forming a primary and secondary segment (C), then a completed rib (D).

The prototype shell is constructed from 30 custom ribs, with each rib fabricated from two laminated layers of 6mm tile 180 to 300mm in depth. Each rib is site-assembled from a staggered configuration of approximately 15 components and acts as a continuous element within the structure (Figure 6). At lap joints between staggered components, only one piece is continuous, while the other is connected with a puzzle-jig type joint. Components were sized to be small enough to nest easily on the material stock, and large enough to maintain a distance of at least one structural bay between adjacent lap joints. Each rib is split into two segments, referred to as a primary and secondary segment. The individual components that comprise each segment are laminated off site using a structural adhesive. 6mm holes in components were used to align corresponding pieces, and were also used to secure pieces together while adhesive cured. The two segments are connected on site via a mechanical bolted joint once both are positioned in the structure. Primary segments overlap primary segments from opposing sides of the structure by approximately 30 cm (Figure 2).

2.2.4 Assembly Process

An important innovation specific to the properties of ceramic tile involved the assembly sequence of the prototype structure. The sequence was geared towards minimizing bending stresses both during construction and upon completion of the structure, as the slender profiles could develop brittle fractures as a result from bending in the weak axis of the rib. During construction, ribs must be installed vertically from above, rather than tilted into place. Once installed, intersecting ribs may bear on one another along the strong axis, but must be free to rotate relative to one another along the weak axis.

The assembly sequence of the rib segments reflects the construction logic of the underlying kagome grid pattern. Rib segments are installed in a radial spiraling pattern from the center outwards (Figure 7). The primary segments are installed following this pattern, which is then repeated for the 30 secondary segments. During construction, the radial assembly sequence facilitates the transport and manipulation of rib segments, and contributes to overall stability of the in-progress structure, as ribs and scaffolding are loaded in a symmetrical fashion. The research team developed a custom CNC cut scaffolding system fabricated from 19mm thick MDF panels that indicated position and assembly order of all ribs. The design of the scaffolding allowed for the incremental decentering of the structure.

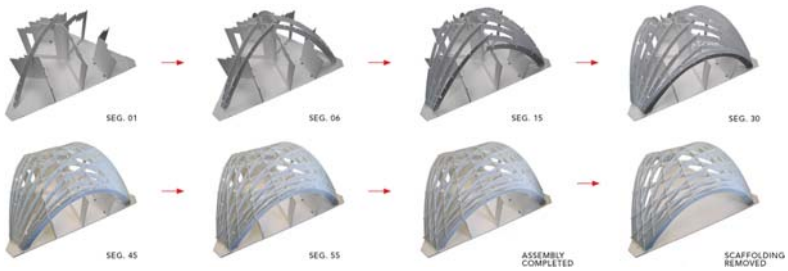

Figure 7: A 1:4 scale prototype was set up to test the feasibility of the assembly sequence.

2.2.5 Connection Detailing

Each rib is slotted to accommodate intersecting rib members, with slot orientations determined by the assembly sequence. Ribs that are installed first have slots on their upper edge to receive subsequent ribs vertically from above. As primary segments are installed first, with only a single notched connection, the majority of their slots are located on the upper edge. Accordingly, the slots of secondary elements are usually located on the lower edge, which enables them to be supported by previously installed elements. Once the primary and secondary segments of a single rib are mechanically fastened together, the now-continuous rib acts as a reciprocal element - supporting any intersecting secondary segments, while simultaneously being supported by any intersecting primary segments. This mutually supportive arrangement satisfies conditions for structural stability, while also allowing each rib to be installed vertically from above, without the need for mechanical connections between ribs.

2.3 Structural Analysis

An analysis model was set up in Multiframe Advanced v17.00.06.0, with each rib modeled as a sequence of straight line segments at the centroid. Grid intersections were modeled with short connecting elements using a rigid connection to one and a pin connection to the other rib. This configuration represents the real nodal constraints while allowing the grid elements themselves to be structurally continuous. All grid supports are pinned.

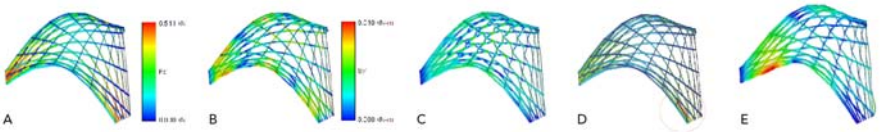

Figure 8: Structural analysis results, including A) Axial forces B) Bending moments C) Deflection D) Buckling Analysis and E) Deformations under combined lateral and gravity loads. Values are shown for self-weight unless otherwise noted.

2.3.1 Member Stresses

The structural analysis deployed a single section profile as the structural element. The grid sections for the system are 2 tiles 6mm thick with varying depth no less than 90mm measured perpendicular to the centroid. For the computational analysis, the section shape for the entire structure was a ceramic tile element 6mm thick and 90mm deep. This is equivalent to the worst case situation at a sheet joint (only one tile continuous) that also includes a notch. The vast majority of locations have much greater sectional capacity.

The loads consist of the self-weight of the ceramic ribs, 2,334 kg/m^3 (145 lbs/ft^3) according to the manufacturer's data. To accommodate any additional fasteners an additional dead load of 0.036 KN/m was applied onto each grid elements. As for lateral loads, no overall wind or seismic loads were modeled since the structure was designed for a secure interior environment. To simulate a person pushing into the structure a lateral load of 1000 N was applied at a height of 1.6m onto a node of the structure (Figure 8E). Member stresses are overall very small (Figure 8A, 8B). Maximum combined bending and axial tensile stresses are 4 MPa – thus well below the allowable strength. Maximum deflections are 0.238 cm with a vertical displacement at the top of the shell midpoint of 0.1 cm (Figure 8C).

Low member stresses in combination with the kagome grid provided sufficient redundancy in case of a local failure of a rib. Ceramic as an extremely brittle material could fracture through impact loads. In that case neighboring ribs are able to take on additional load transfer, and forces can redistribute throughout the grid. When removing 4 short rib segments maximum stresses remained well below 10 MPa.

2.3.2 Member Buckling

The longest member in compression is located near the support (Figure 8D). The effective length of that member is 0.99m (continuous with pin ends). The maximum compression force is 0.277 KN. The cross-section for the buckling analysis assumes the actual 12 x 200mm section, with E = 13,924 MPa as reported in Section 2.1.1. Checking the weak direction shows that the critical buckling load is magnitudes larger than the actual load. $P_{crit} = \pi^2 E I / L_e^2 = 3.14^2$ *13,924 MPa (200mm (6mm)*^{3}*/12) / (990mm)*^{2} *= 504 KN.*

2.3.3 Mechanical Joints

Since 10 ribs radiate from each corner there are a total of 5 different types of construction joints. The analysis assumes 5mm diameter steel bolts are connecting across two tiles. Assume steel bolt M 5 according to ISO 898, property class 4.6 (lowest strength): the long term proof shear load is 3.2 KN, ultimate loads are in the range of 5.6 KN. Assuming an area of 6mm x 5mm the bearing stress on the tile for this load equals F/A = 106 MPa which is higher than the bearing strength. Assuming that bearing and bending strength are equal at 27 MPa the maximum force that can be transferred with a single bolt is *27 MPa = F / (5 x 6mm*^{2}*) > F = 810 N* = 0.81 KN. Assuming a spacing of 2 opposite bolts of 150mm the maximum theoretical moment transfer is equal to *0.81 KN x 0.15m* = 0.122 KN m. From the computational analysis the maximum bending moment at the construction joint is equal to 0.036 KN m. In the final detail the number of bolts were doubled to provide plenty of spare capacity to carry the bending moments and increase rigidity.

3. Fabrication and Construction

Rib segments were CNC waterjet cut and pre-assembled in the shop. Several pieces broke at their weakest areas – mostly near bolt holes, or near the connection slots. Fractures occurred prior to lamination and whenever bending was unintentionally induced in the weak direction of the rib. Special care had to be taken in transporting cut pieces to the lamination shop. No fractures were recorded in laminated rib segments on site.

Ceramic is dimensionally extremely stable with respect to moisture or temperature fluctuations – and in that respect differs from wood and metal. Given the precision of CNC waterjet cutting, construction tolerances at each joint were only 2.5mm per side. The base support was carefully built to maximum precision, and assembly was completed without any re-cutting or adapting of ribs. Upon completion of construction, vertical deflection of the structure was measured at the three centermost rib intersections and found to be within 9mm of the design values.

4. Conclusion

Although continuous shells have been built using ceramics, grid shells are most typically built using steel or timber, and on occasion concrete. The paper investigates the feasibility of ceramics as a primary structural material for grid shell systems, with a particular focus on large format ceramic tiles. Certain attributes of ceramics, such as resistance to fire, mildew and pests make the material a promising choice over other standard construction materials where durability and sanitary conditions might be desirable. In addition, the capacity for being glazed and printed on may expand the aesthetic possibilities of grid shells.

The paper presents a dedicated design and manufacturing workflow for ceramic grid shells. Material and joint tests determined the design values used in the structural analysis. A limitation of ceramic structural elements was found to be the risk of fractures during transport and fabrication. The combination of large safety margins in the final structure along with system redundancy through the

choice of the kagome grid pattern contributed to realizing an overall safe design. The geometric pattern, joinery and sequence of assembly reflected principles of shell construction, as well as considerations specific to the properties ceramic tile. As such, this work constitutes a promising development in the implementation of ceramics as a material for the construction of grid shells.

Acknowledgements

The authors thank ASCER Tile of Spain for their continuing support. Cevisama 2018 provided additional support for the exhibition. Javier Mira from the Instituto de Tecnología Cerámica as well as Groupo on Market helped realize the design.

References

[1] M. Bechthold, A. Kane, and N. King: Ceramic Material Systems. Basel: Birkhäuser, 2015.

[2] E. Sánchez, J. García-Ten, V. Sanz, and A. Moreno, "Porcelain tile: Almost 30 years of steady scientific-technological evolution," Ceramics International, vol. 36, no. 3, pp. 831–845, Apr. 2010.

[3] M. Bechthold, "Ceramic Prototypes - Design, Computation, and Digital Fabrication," Informes de la Construcción, vol. 68, no. 544, Dec. 2016.

[4] J. Ochsendorf, Guastavino Vaulting: The Art of Structural Tile. New York: Princeton Architectural Press, 2013.

[5] E. Dieste, Eladio Dieste: La Estructura Cerámica. Colombia: Escala, 1987.

[6] M. Bechthold, Innovative Surface Structures: Technologies and Applications. London: Taylor & Francis, 2008.

[7] S. Anderson, Eladio Dieste: Innovation in Structural Art. Princeton Architectural Press, 2004.

[8] D. López López, T. Van Mele, and P. Block, "Dieste, González Zuleta and Sánchez del Río: Three approaches to reinforced-brick shell structures," in Structural Analysis of Historical Constructions: Anamnesis, Diagnosis, Thera-py, Controls, London, 2016.

[9] L. Davis, M. Rippmann, T. Pawlofsky, and P. Block, "Efficient and expressive thin-tile vaulting using cardboard formwork," Proceedings of the IABSE-IASS Symposium 2011, 2011.

[10] P. Block, T. van Mele, M. Rippmann, and N. Paulson, Beyond Bending: Re-imagining Compression Shells. Munich: Detail, 2017.

[11] S. Adriaenssens, P. Block, D. Veenendaal, and C. Williams, Eds.: Shell Structures for Architecture: Form Finding and Optimization. London: Routledge, 2014.

[12] J. Chilton and G. Tang, Timber Gridshells: Architecture Structure and Craft. London: Routledge, 2016.

[13] P. Jodido, Shigeru Ban: Complete Works 1985-2015. Cologne: Taschen, 2015.

[14] R. Mesnil, C. Douthe, and O. Baverel: "Non-Standard Patterns for Gridshell Structures: Fabrication and Structural Optimization," Journal of the International Association for Shell and Spatial Structures, International Association for Shell and Spatial Structures, vol. 58, no. 4, pp. 277–286, 2017.

[15] R. Mesnil, C. Douthe, O. Baverel, and B. Leger: "Linear buckling of quadrangular and kagome gridshells: a comparative assessment," Engineering Structures, no. 132, pp. 337–348, Feb. 2017.

[16] H. Schaal, Lineare Algebra und analytische Geometrie, Band II. Berlin: Vieweg, 1980